Chinese Physics C Vol. 40, No. 9 (2016) 098102

Self-seeded FEL wavelength extension with high-gain harmonic generation

Ling Zeng(曾凌)[1] Weilun Qin(秦伟伦)[1] Gang Zhao(赵刚)[1] Senlin Huang(黄森林)[1;1)]
Yuantao Ding[2] Zhirong Huang[2] Gabriel Marcus[2] Kexin Liu(刘克新)[1]

[1] Institute of Heavy Ion Physics, School of Physics, Peking University, Beijing 100871, China
[2] SLAC National Accelerator Laboratory, Menlo Park, CA 94025, USA

Abstract: We study a self-seeded high-gain harmonic generation (HGHG) free-electron laser (FEL) scheme to extend the wavelength of a soft X-ray FEL. This scheme uses a regular self-seeding monochromator to generate a seed laser at the wavelength of 1.52 nm, followed by a HGHG configuration to produce coherent, narrow-bandwidth harmonic radiations at the GW level. The 2nd and 3rd harmonic radiation is investigated with start-to-end simulations. Detailed studies of the FEL performance and shot-to-shot fluctuations are presented.

Keywords: FEL, self-seeding, HGHG

PACS: 41.60.Cr, 41.75.Ht, 42.65.Ky **DOI:** 10.1088/1674-1137/40/9/098102

1 Introduction

X-ray free electron lasers (FELs), which demonstrate an improvement in peak brightness of approximately ten orders of magnitude over third-generation light sources, have shown remarkable scientific capabilities in chemistry, biology, material science, as well as many other disciplines. There are two main schemes for single pass short wavelength FELs: self-amplified spontaneous emission (SASE) [1, 2] and high-gain harmonic generation (HGHG) [3, 4]. Until recently, most modern high-gain FELs in the short wavelength (e.g., X-ray) region, such as the LCLS and the SACLA FEL [5, 6], have been operated in SASE mode, which is characterized by excellent transverse coherence. However, SASE FELs have poor temporal coherence and large shot-to-shot fluctuations in both the time and frequency domains, since they start from shot noise [7].

HGHG FELs can generate fully coherent, high gain harmonic radiation from a seed laser. However, the harmonic number (n) of a single-stage HGHG FEL is limited by the requirement that the induced energy spread be less than the Pierce parameter (ρ) in the radiation undulator (radiator) to achieve high gain. So far, the highest harmonic obtained with single-stage HGHG is the 13th harmonic at 20 nm using a 1.2 GeV electron beam at FERMI [8]. In order to reach higher harmonics, so as to obtain shorter wavelength fully coherent FEL, several schemes have been proposed in recent years. Among them, the cascaded HGHG scheme with the help of the "fresh bunch" technique was proposed in 2001 [9]. Recently, 4.3 nm radiation (60th harmonic of a 260 nm UV seed laser) has been achieved with a two-stage HGHG configuration at FERMI [10]. One other scheme, EEHG [11], was first proof-of-principle demonstrated at SLAC [12]. In 2011, researchers from Shanghai Institute of Applied Physics (SINAP) also observed the third harmonic from EEHG, which was further amplified to saturation [13]. Currently, EEHG at 160 nm (15th harmonic of a 2400 nm seed laser) has been produced at SLAC [14]. However, the cascaded HGHG and EEHG still have difficulty in generating hard X-ray FELs due to a lack of external seeds at X-ray wavelengths [15].

To solve the difficulty of external seeding at very short wavelengths, colleagues at DESY proposed an approach of self seeding in 1997 [16], and recently a simplified monochromator version for hard X-rays [17]. This self-seeded FEL starts from a SASE stage, which operates in the linear regime. A following monochromator is used to generate a purified seed from the SASE radiation, and meanwhile the electron beam after the SASE stage goes through a bypass chicane. They recombine in an amplification undulator (amplifier stage) for further interaction, where the seed radiation gets amplified to saturation, producing near Fourier transform limited X-rays. The self-seeding approach works for both soft and hard X-ray FELs and has been successfully demonstrated recently [15, 18]. It is worth noticing that two different configurations of monochromator have been used depending on the spectral range. For X-ray FELs

Received 7 April 2016, Revised 6 May 2016
1) E-mail: huangsl@pku.edu.cn

with the photon energy below 2 keV, a grating-based monochromator has been used [15], while for X-ray FELs with the photon energy above 4.5 keV, a diamond-based monochromator is more popular [18]. Within the photon energy range from 2 keV to 4.5 keV, the self-seeded FEL is difficult due to a lack of monochromator materials. This motivates to study alternative schemes to cover the energy gap from 2 – 4.5 keV.

In this paper, we study a new scheme combining the self-seeding approach with HGHG to produce fully coherent X-rays. It can not only fill the above photon energy gap not easily achieved by regular self-seeded FELs, but also extend the wavelength of a soft X-ray FEL machine to the harder X-ray region. This self-seeded HGHG scheme will be described in Section 2, followed by the FEL simulation results in Sections 3 and 4.

2 Self-seeded HGHG Scheme

The proposed setup of the self-seeded HGHG scheme is shown in Fig. 1. It consists of two stages: the SASE stage and the HGHG stage. The SASE stage follows the regular self-seeding configuration, comprising a SASE undulator, an X-ray monochromator, and an electron beam bypass chicane allowing room for the monochromator. An electron beam first traverses the SASE undulator, generating SASE radiation in the linear regime. After the SASE undulator, the radiation goes through the X-ray monochromator, which transmits a narrow band of wavelengths. The transmitted radiation is then used as a seed for the following FEL amplifier. Meanwhile, the electron beam from the SASE undulator goes through a bypass chicane, being properly delayed, and recombines with the seed radiation at the entrance of the HGHG stage. The bypass chicane also helps to wash out the microbunching of the electron beam built up in the SASE undulator.

Compared to the external seed laser in the regular HGHG scheme, the seed radiation from the SASE stage has a much lower power, limited to a few hundred kilowatts because of the damage threshold of the state-of-the-art X-ray monochromator optics [15]. As a result, we need to use a long modulation undulator with two combined functions. The first function is to amplify the seed radiation from the SASE stage, which is mainly achieved with the upstream part of the modulation undulator. The second is to introduce energy modulation to the electron beam, as in a normal HGHG modulator. The energy modulated electron beam then goes through the dispersion chicane with proper R_{56}, getting density modulated, and radiates at the harmonic wavelength of the seed.

In this self-seeded HGHG scheme, the electron beam quality inevitably degrades when it is used to amplify the seed radiation from the SASE stage. Therefore a compromise should be made between the modulation radiation power and the induced electron energy spread growth in the HGHG modulator. In this paper, the modulation laser power is kept at hundred megawatt level to avoid a significant energy spread degradation of the electron beam in the seed amplification process.

To eliminate the impact of electron energy spread degradation in the seed amplification process, we have also proposed a self-seeded HGHG FEL setup with separated seed amplifier and modulator (see Fig. 2). In this case an electron beam with longer bunch length is used, which generates double-spike seed after the X-ray monochromator. The head spike of the seed is then aligned with the tail part of the electron bunch at the entrance of the amplifying undulator (U_A). Therefore only the tail part of the electron bunch is used to amplify the seed while the head part is kept undisturbed and "fresh". After the U_A undulator, the electron bunch is delayed by a small chicane (C_{B2}), and consequently the head part is aligned with the seed radiation in the modulation undulator (U_{M2}) and gets energy-modulated. After the U_{M2} undulator, the electron beam undergoes the same procedure as the above setup.

In the following discussions, the first setup is referred to as the long modulator case, while the second setup is referred to as the "fresh bunch" case.

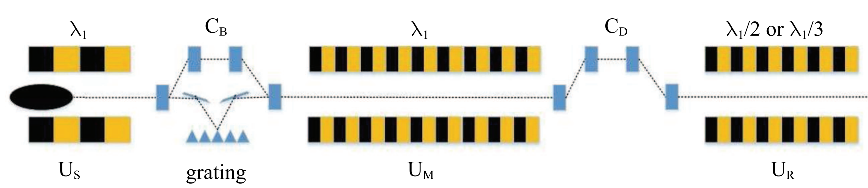

Fig. 1. Schematic of self-seeded HGHG FEL. U_S is a SASE undulator, U_M is a long modulation undulator with combined functions as seed amplifier and HGHG modulator, and U_R is a radiation undulator (radiator) of HGHG. C_B is a bypass chicane steering the electron beam around the X-ray monochromator, while C_D is a dispersion chicane of the HGHG stage.

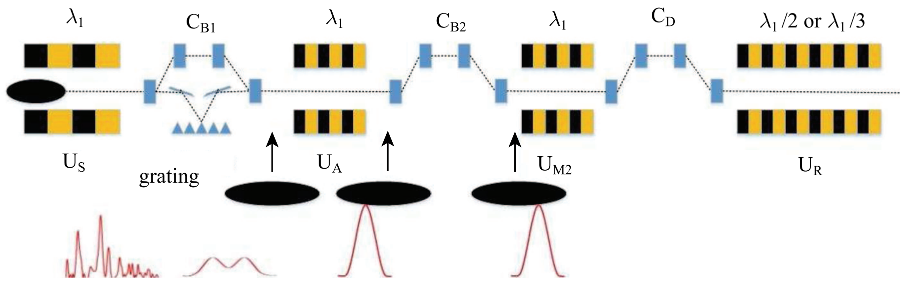

Fig. 2. Self-seeded HGHG FEL with separated seed amplifier (using U_A undulator) and modulator (using U_{M2} undulator). C_{B2} is an electron delay chicane.

3 FEL simulation of long modulator case

As a representative example, we use the soft X-ray self-seeded (SXSS) FEL at LCLS to illustrate the feasibility of this scheme. Parameters are assumed based on the SXSS FEL for time-dependent FEL simulation using GENESIS [19] code. The electron beam has a central energy of 4.3 GeV, an uncorrelated energy spread of 1.0 MeV, and a normalized transverse emittance of 0.5 mm-mrad. It has a uniform current profile with a pulse duration of 30 fs and peak current of 2.5 kA. The SASE undulator (U_S) is resonant at 1.52 nm. It uses 5 LCLS undulator segments and has a total length of 19.8 m (including the focusing optics in between). This is based on the consideration of keeping the SASE FEL power at the highest level while avoiding damage to the X-ray monochromator optics. The monochromator is assumed to have a Gaussian spectral response with a maximum power efficiency of 0.02 at 1.52 nm. An example of the FEL power profiles and power spectra after the SASE undulator and X-ray monochromator is shown in Fig. 3. One can see from the figure that after the monochromator the radiation peak power drops to about 220 kW while a narrow bandwidth is filtered out.

For the HGHG modulator, an optimal value for the electron energy modulation amplitude $\Delta\eta_m$ is [3, 4]

$$\Delta\eta_m \approx n\sigma_\eta, \tag{1}$$

with σ_η the intrinsic uncorrelated energy spread and n the harmonic number. In order to obtain the optimal energy modulation, the length of U_M undulator needs to be optimized. Herein we study the 2nd and 3rd harmonic generation and accordingly the undulator length is chosen to be 13 m and 14 m, respectively, to meet the above criteria of optimized energy modulation amplitude.

The momentum compaction factor R_{56} of the chicane C_D is set to satisfy [11]

$$R_{56}\Delta\gamma_m/\gamma \approx \lambda/4, \tag{2}$$

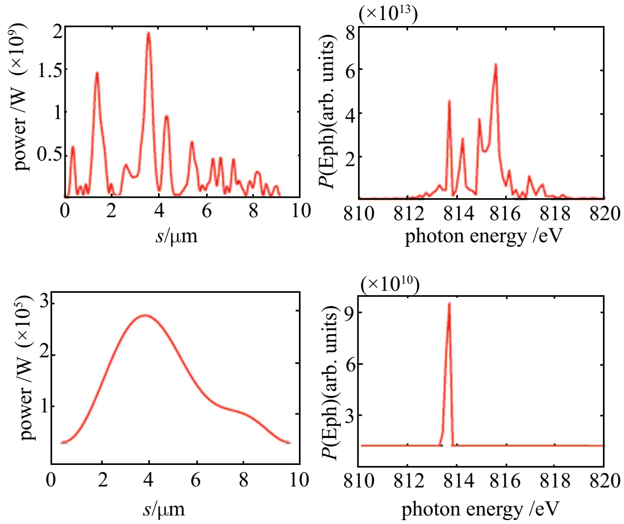

Fig. 3. FEL power profiles (left) and spectra (right) at the exit of U_S undulator (top) and after monochromator (bottom) in the long modulator case.

where λ is the wavelength of the seed laser. In this long modulator case, the value of R_{56} are 0.56 μm and 0.46 μm for the 2nd and 3rd harmonic generation, respectively. The longitudinal phase space of electron beam after the modulation undulator (U_M) and dispersion chicane are shown in Fig. 4.

The main electron and radiation parameters used in this study are summarized in Table 1. With these parameters, GENESIS simulations were performed. Figure 5 illustrates the evolution of the FEL power of the 2nd and 3rd harmonic radiation along the radiation undulator. We can see from the figure that the 2nd harmonic radiation at the exit of the radiation undulator is about 3.6 GW, while the 3rd harmonic radiation is about 0.9 GW. Figure 6 shows the output power profile and spectra of the 2nd and 3rd harmonic radiation at the exit of the radiation undulator, which indicate that the normalized spectral width (FWHM) of the 2nd and 3rd harmonic are 1.8×10^{-4} and 1.5×10^{-4} respectively.

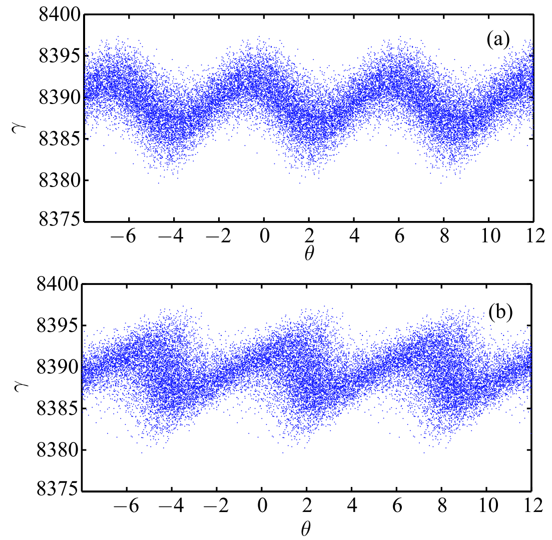

Fig. 4. Longitudinal phase space evolution in HGHG based on the self-seeding scheme. (a) At the exit of modulator U_M; (b) At the exit of dispersion section C_D.

Table 1. Electron and radiation parameters used in the FEL study of the long modulator case.

parameter	value	unit
electron beam		
energy	4.3	GeV
energy spread	1.0	MeV
peak current	2.5	kA
bunch length (full width)	30	fs
normalized emittance	0.5	mm-mrad
radiation		
undulator period	3	cm
U_S undulator length	19.8	m
U_M undulator length (2nd/3rd)	13/14	m
U_R undulator length (2nd/3rd)	25/33	m
mono. central wavelength	1.52	nm
mono. resolving power	5000	
mono. power efficiency	0.02	
bypass chicane R_{56}	−0.4	mm
disp. chicane R_{56} (2nd/3rd)	−0.56/−0.46	µm
FEL wavelength (2nd/3rd)	0.76/0.51	nm

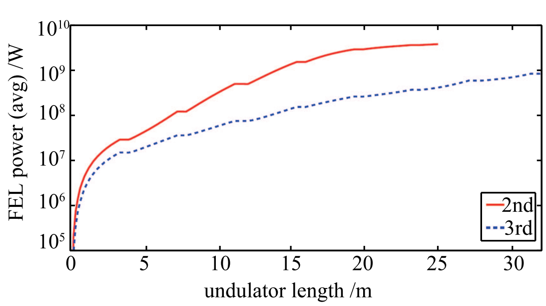

Fig. 5. Average power evolution in the U_R undulator in the long modulator case.

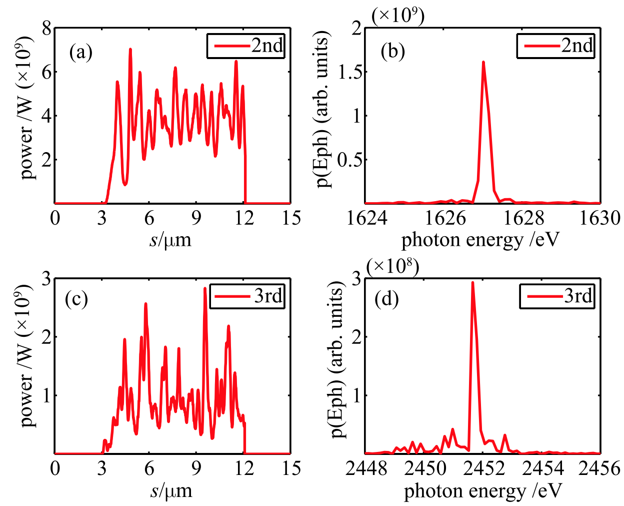

Fig. 6. The FEL output power profile and spectrum of the self-seeding HGHG scheme in the long modulator case.

4 FEL simulation of "fresh bunch" case

To generate the desired seed after the X-ray monochromator, a 60 fs long electron bunch is used, which is twice that used in the long modulator case. Other electron parameters are kept unchanged, as in Table 1. The SASE undulator (U_S) and the X-ray monochromator remain the same as in the long modulator case.

An example of the FEL power profiles and power spectra after the SASE undulator and X-ray monochromator is shown in Fig. 7. As shown in the figure, the temporal profile of the seed has double spikes. The head spike of the seed is then aligned with the tail part of the electron bunch at the entrance of the amplifying undulator (U_A) by fine-tuning the bypass chicane (C_B) at µm level. The seed radiation copropagates with the electron bunch in the undulator and gets amplified. The length of U_A undulator is chosen based on the consideration that the seed laser power can be amplified as much as possible while keeping the head part of the electron bunch fresh. In this case, the U_A undulator length is 11 m. The evolution of the seed radiation pulse and electron bunch in U_A is shown in Fig. 8. It can be seen from the figure that, while the peak power of the radiation is amplified to about 100 MW in the U_A undulator, the head electrons in the bunch do not get disturbed. It is obvious that the energy spread of the tail electrons becomes larger, however, it is also worth noting that the energy spread increase is not significant.

After the U_A undulator, the electron bunch is delayed by the C_{B2} chicane, and the head part electrons are aligned with the seed radiation in the U_{M2} modulation undulator. The length of U_{M2} undulator is optimized according to Eq. (1). For the 2nd and 3rd harmonic generation, the undulator length is chosen to be 2.5 m and 3.5 m, respectively. The dispersion chicane C_D in this "fresh bunch" case has an R_{56} of 0.50 μm and 0.42 μm for the 2nd and 3rd harmonic generation, respectively, according to Eq. (2).

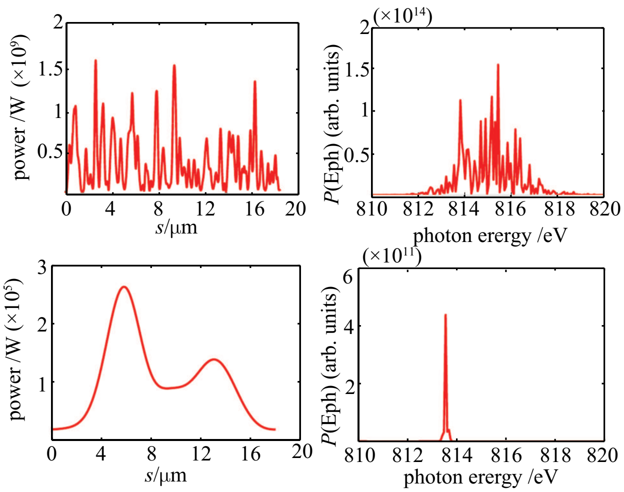

Fig. 7. FEL power profiles (left) and spectra (right) at the exit of U_S undulator (top) and after the monochromator (bottom) in the "fresh bunch" case.

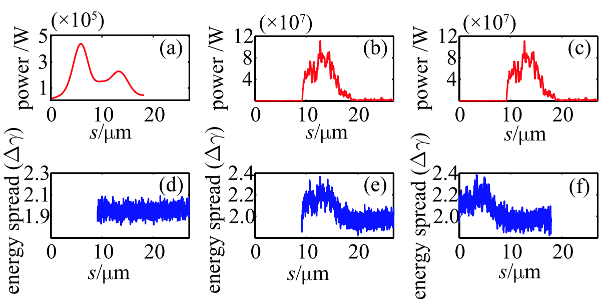

Fig. 8. Simulated radiation power (top) and electron beam (bottom) evolution at the entrance to U_A (left), at the exit of U_A (middle) and at the entrance to U_{M2} (right) in the "fresh bunch" case.

Figure 9 shows the evolution of the FEL power of the 2nd and 3rd harmonic radiation along the radiation undulator. The length of the radiation undulator U_R is 20 m and 28 m, respectively. As shown in the figure, the 2nd harmonic radiation at the exit of the radiation undulator is about 7.8 GW, and the 3rd harmonic radiation has a power of about 1.9 GW.

The output power profile and spectra of the 2nd and 3rd harmonic radiation at the exit of the radiation undulator are shown in Fig. 10, which demonstrate that the normalized spectral width (FWHM) of the 2nd and 3rd harmonic are 1.6×10^{-4} and 1.4×10^{-4} respectively.

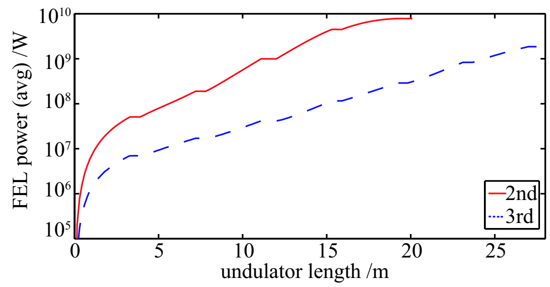

Fig. 9. Average power evolution in the U_R undulator in the "fresh bunch" case.

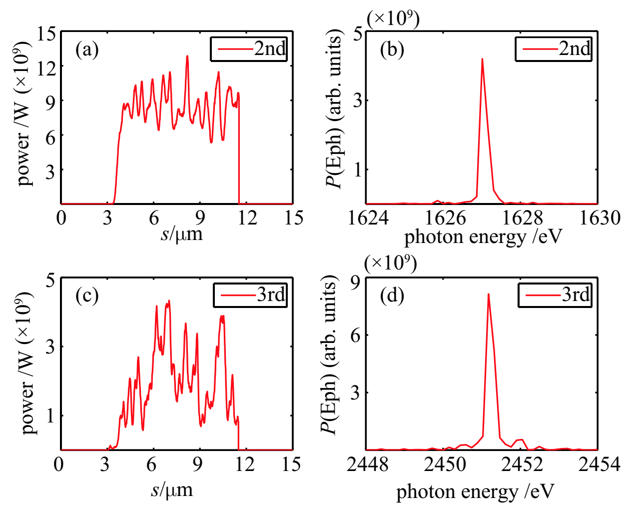

Fig. 10. The output power profile and spectrum of the self-seeding HGHG scheme in the "fresh bunch" case.

To analyze the statistical fluctuation on the radiation pulse, a series of 10 separate GENESIS runs have been performed, distinguished by different random shot noise initialization of the SASE radiation in the U_S undulator. The statistical average output power for the 2nd and 3rd harmonic in the long modulator case are 2.3 GW and 0.7 GW respectively, while those in the fresh bunch case are 5.6 GW and 1.7 GW respectively. The shot-to-shot output power fluctuation of the 2nd and 3rd harmonic are 33.27% (RMS) and 30.40% (RMS) respectively in the long modulator case, and 36.16% (RMS) and 38.98% (RMS) respectively in the "fresh bunch" case.

5 Conclusion

In this paper, we have proposed a self-seeded HGHG scheme, which may be an attractive way to extend regular self-seeded FELs to shorter wavelengths, especially within the photon energy range from 2 keV to 4.5 keV, which is difficult to achieve due to a lack of monochromator materials. This method is also applicable to extend hard X-ray self-seeding with crystals to even shorter wavelengths. We use parameters based on the SXSS FEL at LCLS to simulate the scheme in two cases. In the long modulator case, we obtained 2nd harmonic with FEL power 2.3 GW and normalized spectral width (FWHM) 1.8×10^{-4}, and 3rd harmonic with FEL power 0.7 GW and normalized spectral width 1.5×10^{-4}. In the "fresh bunch" case, we obtained 2nd harmonic with FEL power 5.6 GW and normalized spectral width 1.6×10^{-4}, and 3rd harmonic with FEL power 1.7 GW and normalized spectral width 1.4×10^{-4}.

Note that in these demonstration examples, we chose a fundamental energy at 810 eV to calculate the second and third harmonic performance. The soft X-ray self-seeding setup can work at 1.5 keV fundamental energy with the same monochromator, so we can scale up to reach 4.5 keV at the third harmonic to cover the energy gap we discussed earlier. Also, we used a conserved energy spread of 1 MeV rms based on the present LCLS operation parameters. A lower energy spread is possible based on LCLS-II design studies, which should help the harmonic performance. This will be investigated in the future.

References

1 A. M. Kondratenko and E. L. Saldin, Part. Accel, **10**: 207–216 (1980)
2 R. Bonifacio, C. Pellegrini, and L. M. Narducci, Optics Communications, **50** (6): 373–378 (1984)
3 I. Ben-Zvi et al, Nucl. Instrum. Methods. A, **304**: 181 (1991)
4 L. Yu, Phys. Rev. A, **44**: 5178 (1991)
5 P. Emma, R. Akre, J. Arthur et al, Nature Photonics, **4** (9): 641–647 (2010)
6 T. Ishikawa, H. Aoyagi, T. Asaka et al, Nature Photonics, **6** (8): 540–544 (2012)
7 Z. Huang and K. J. Kim, Phys. Rev. ST. Accel. Beams, **10**: 034801 (2007)
8 E. Allaria et al, Nature Photonics, **6**: 699 (2012)
9 J. Wu and L. Yu, Nucl. Instrum. Methods. A, **475**: 104–111 (2001)
10 E. Allaria et al, Nature Photonics, **7** (11): 913–918 (2013)
11 D. Xiang and G. Stupakov, Phys. Rev. ST. Accel. Beams, **12** (3): 030702 (2009)
12 M. Dunning et al, A proof-of-principle Echo-enabled Harmonic Generation FEL Experiment at SLAC, in *Proceedings of the 1st International Particle Accelerator Conference* (Kyoto, 2010), p. 2293–2295
13 Z. T. Zhao, D. Wang, J. H. Chen et al, Nature Photonics, **6** (6): 360–363 (2012)
14 E. Hemsing, M. Dunning, C. Hast et al, Phys. Rev. ST. Accel. Beams, **17**: 070702 (2014)
15 D. Ratner, R. Abela, J. Amann et al, Phys. Rev. Lett, **114** (5): 054801 (2015)
16 J. Feldhaus, E. L. Saldin, J. R. Schneider et al, Optics Communications, **140** (4): 341–352 (1997)
17 G. Geloni, V. Kocharyan, and E. L. Saldin, Journal of Modern Optics, **58** (16): 1391–1403 (2011)
18 J. Amann et al, Nature Photonics, **6**: 693–698 (2012)
19 S. Reiche, Nucl. Instrum. Methods A, **429**: 243 (1999)